electrochem

MDPI

Article

Biofilm Activity of *Shewanella oneidensis* on Gold Electrodes Monitored by Electrochemical Surface Plasmon Resonance Imaging (eSPRi)

Lina J. Bird, Joel P. Golden, Rebecca L. Mickol, Zachary T. Johnson, Matthew D. Yates and Scott A. Trammell *

U.S. Naval Research Laboratory, 4555 Overlook Avenue SW, Washington, DC 20375, USA; rebecca.l.mickol.civ@us.navy.mil (R.L.M.); zachary.t.johnson120.civ@us.navy.mil (Z.T.J.); matthew.d.yates7.civ@us.navy.mil (M.D.Y.)

* Correspondence: scott.a.trammell2.civ@us.navy.mil; Tel.: +1-202-404-6063

Abstract

This study investigates the use of electrochemical surface plasmon resonance imaging (eSPRi) to monitor the growth and activity of *Shewanella oneidensis* biofilms on gold film electrodes. Motivated by the need to understand extracellular electron transfer (EET) in biofilms, particularly the roles of surface-attached and soluble redox-active molecules, we aimed to correlate eSPRi data with electrochemical measurements during biofilm development. The combined measurements revealed distinct phases of biofilm behavior, including an initial period in which current and eSPRi signal increased together, followed by later phases in which current declined while the eSPRi signal remained elevated or increased. These findings highlight the complexity of biofilm-electrode interactions and demonstrate the value of eSPRi as a complementary tool for studying microbial electrochemical interfaces. Ultimately, this work paves the way for more nuanced explorations of microbial–electrode interfaces, with potential payoffs in the optimization of bioelectrochemical technologies.

Keywords: *Shewanella oneidensis*; electrochemical surface plasmon resonance imaging (eSPRi); biofilm formation; extracellular electron transfer; gold electrodes

1. Introduction

The bacterium *Shewanella oneidensis* is well-known for its ability to transfer electrons to a solid electrode via multiheme cytochromes or soluble flavins [1–5]. Despite extensive research, important aspects of its interaction with electrode surfaces remain unclear, particularly the relative contributions of surface-attached and soluble redox-active species to extracellular electron transfer. Studies have shown that electrode potential can regulate cytochrome accumulation on the cell surface of *Shewanella oneidensis*, impacting bioelectrocatalytic current generation [1]. Additionally, there is evidence suggesting that flavins can influence the rate of electron transfer to electrodes [2]. Previous work has also distinguished the roles of free and cytochrome-bound flavins in extracellular electron transport [3]. These studies have shown that flavins can interact with the electrode both as diffusible shuttles and complexed with multi-heme cytochromes. The electrode material appears to influence which reaction is dominant.

In these studies, electrochemical methods such as chronoamperometry and cyclic voltammetry are primarily utilized to study extracellular electron transfer (EET) in electroactive biofilms on electrodes. Chronoamperometry characterizes growth rate and maximum

Check for updates

Academic Editor: Michael Lyons

Received: 26 June 2026
Revised: 18 August 2026
Accepted: 20 September 2026
Published: 23 September 2026

Copyright: © 2026 by the authors. Licensee MDPI, Basel, Switzerland. This article is an open access article distributed under the terms and conditions of the Creative Commons Attribution (CC BY) license.

sustained current activity [6] while cyclic voltammetry and differential pulse voltammetry can help determine the underlying electron transfer mechanism [7]. Alternatively, Golden et al. previously showed that electrochemical surface plasmon resonance imaging (eSPRi) offers an optical approach to interrogate extracellular electron transfer in biofilms since eSPRi is sensitive to changes in refractive index at the interface between an aqueous solution and the electrode surface [8]. eSPRi's short depth of sensitivity, typically within tens to hundreds of nanometers, results in high signal-to-noise measurements of interfacial processes [8]. This technique simultaneously employs the conducting surface as a working electrode, allowing optical monitoring of electrochemical and interfacial changes via changes in local refractive index near the electrode [8]. In biofilm systems, these optical changes may reflect contributions from redox-state changes, biomass accumulation, extracellular material, and other interfacial processes.

One complicating factor in using this technique is the requirement that the electrode material be gold. Although *S. oneidensis* produces current on gold [9], it does so at a much lower rate than on carbon electrodes. Because eSPRi requires a gold film substrate, the present study examines a biofilm-electrode interface that may not be optimal for sustained extracellular electron transfer by *S. oneidensis*. This constraint is important when interpreting both the electrochemical and optical responses, as direct electrochemistry of cytochromes on bare, unmodified gold can often yield weak, irreversible, or adsorption-related features. Nevertheless, the use of eSPRi can provide valuable information about the electrode-molecular interface.

Although eSPRi has been applied to electroactive biofilms, its ability to track the development and changing activity of biofilms on gold electrodes remains underexplored. Here, we use eSPRi to examine how interfacial optical signals evolve during biofilm growth and how those signals relate to current production.

2. Materials and Methods

2.1. Materials

Medium components were purchased from Sigma-Aldrich unless otherwise indicated. Gold eSPRi slides were purchased from Platypus Technologies (Madison, WI, USA), and the eSPRi instrument was purchased from GWC Technologies (Madison, WI, USA).

Shewanella basal medium contained, per liter: 0.46 g NH_4Cl, 0.225 g K_2HPO_4, 0.225 g KH_2PO_4, 0.117 g $MgSO_4 \cdot 7H_2O$, 0.225 g $(NH_4)_2SO_4$, 23.8 g HEPES, 25 mM lactate, 0.1% casamino acid, 5 mL of mineral mix ([per liter]: 1.5 g nitrilotriacetic acid, 0.1 g $MnCl_2$ $4H_2O$, 0.3 g $FeSO_4 \cdot 7H_2O$, 0.17 g $CoCl_2 \cdot 6H_2O$, 0.1 g $ZnCl_2$, 0.04 g $CuSO_4 \cdot 5H_2O$, 0.005 g $AlK(SO_4)_2 \cdot 12H_2O$, 0.005 g H_3BO_3, 0.09 g Na_2MoO_4, 0.12 g $NiCl_2$, 0.02 g $NaWO_4 \cdot 2H_2O$, 0.10 g Na_2SeO_4, and 5 mL of vitamin mix [per liter]: 0.002 g biotin, 0.002 g folic acid, 0.02 g pyridoxine HCl, 0.005 g thiamine, 0.005 g nicotinic acid, 0.005 g pantothenic acid, 0.0001 g B-12, 0.005 g p-aminobenzoic acid, 0.005 g thioctic acid. The lactate, vitamin mix, and casamino acid were added after autoclaving.

2.2. Shewanella oneidensis Biofilm Cultivation

S. oneidensis MR1 was inoculated from a Luria–Bertani (LB) agar plate into 5 mL LB liquid medium and grown overnight at 30 °C. The next day, 0.5 mL of the culture was pelleted, rinsed once, and resuspended in Shewanella basal medium. This inoculum was then injected into the deoxygenated eSPRi cell with the gold electrode poised at 0.31 V vs. SHE. The biofilm was allowed to develop at room temperature under a nitrogen gas sparge for 12 h before the first cyclic voltammogram (CV) was recorded. During this time, the development of current was monitored, and samples for lactate analysis were taken during active current production and again after current production had decreased.

2.3. SPR Setup and Electrochemical Conditions

We have reported the electrochemical surface plasmon resonance imaging (eSPRi) setup in a previous paper [8]. The eSPRi instrument was set to take an image every 30 s over the course of the experiment. The gold eSPRi slide served as the working electrode and was connected to the potentiostat using a wire soldered with low-temperature indium solder to avoid damaging the thin gold layer. A small amount of epoxy on the connection provided strain relief. The chamber exposed 3.14 cm^2 of the working electrode surface area. The counter electrode was a graphite rod, and the reference electrode was 1 M Ag/AgCl. The electrode was poised, and electrochemical data were collected using a Gamry potentiostat. The gold slides were plasma-cleaned before use, then rinsed with water. Each slide's gold layer was scored before placing it in the eSPRi holder to create a built-in open-circuit control region for each experimental run. This setup helped differentiate potential-dependent interfacial changes from general optical or bulk effects. The slide was placed in the holder, and the whole setup was rinsed with ethanol for sterilization, then rinsed with sterile water before adding sterile minimal medium. Nitrogen was bubbled into the medium using a bent cannula, with a raised exit point to avoid splashing medium into the exit needle. After nitrogen flow began, rapid CVs were performed to verify the loss of the oxygen reduction signal, indicating that the reactor chamber was becoming anaerobic.

2.4. Data Synchronization and Analysis

Because the eSPRi data were collected as a series of images using separate software from that used to collect electrochemical signals from the potentiostat, the two datasets had to be synchronized. This was performed using R to extract the timestamps from the TIFF images collected by the eSPRi instrument and synchronize them with the electrochemical data files recorded by the potentiostat. Because the eSPRi imaging was initiated first, the timestamp of the first image was used as the origin time, and the elapsed time for both data types was calculated based on the origin time. Each image from the eSPRi was divided into grids, and the area in each grid was averaged for each time point to allow comparison between different regions of the slide. Data presented here were extracted primarily from a representative region near the center of the active area (e.g., square 45), reflecting distinct localized temporal behavior.

2.5. Lactate Analysis

Samples were removed from the SPR chamber and sterile-filtered (0.22 μm, 25 mm, PES, part #76479-024, VWR International, Radnor, PA, USA) into 2 mL HPLC vials (part #5182-0716, Agilent Technologies, Santa Clara, CA, USA) with screw caps (part #5190-7021, Agilent) to quantify lactate concentration. For the creation of standards, a stock solution of 100 mM lactate was prepared in basal Shewanella medium without lactate. The stock solution was acidified to pH 2 with 18.7 M sulfuric acid (H_2SO_4; sulfuric acid 98%, for HPLC LiChropur, part #5438270250, Supelco, Bellefonte, PA, USA) (ca. 5 μL/mL) and sterile-filtered into a 50 mL centrifuge tube. Using the acidified 100 mM lactate stock solution and acidified basal Shewanella medium (containing no carbon source), standards were created at ten concentrations (100 mM, 50 mM, 25 mM, 10 mM, 5 mM, 1 mM, 0.5 mM, 0.25 mM, 0.1 mM, 0.05 mM) by serial dilution. Lactate was quantified via HPLC (Agilent 1260 Infinity II) with a diode array detector at 210 nm. The column was a Hi-Plex H (300 × 6.5 mm, part #PL1F70-6830, Agilent). The mobile phase was 5 mM H_2SO_4, and the flow rate was 0.4 mL/min. The column compartment was set to 55 °C. Lactate eluates were collected at 14.7 min, and the R^2 value of the standard curve was 0.9999.

3. Results

3.1. Biofilm Activity Monitored by eSPRi and Electrochemistry

Our primary goal was to characterize *S. oneidensis* biofilm growth on a gold-film electrode and determine whether eSPRi could be used to monitor interfacial changes associated with biofilm development and electrochemical activity optically. Specifically, we aimed to investigate whether optical changes measured by eSPRi could be correlated with electrochemical behavior at the biofilm-gold interface. To achieve this, we designed experiments to correlate eSPRi data with current data measured by the potentiostat. A schematic of the experiments is shown in Figure 1A. Both measurements were recorded simultaneously, with the potentiostat programmed to conduct a series of experiments driving the electrochemical measurements. This series of experiments included two short chronoamperometry pulses to validate the synchronization of the eSPRi data and the electrochemical data. The experiments consisted of a long-time course of chronoamperometry to promote biofilm growth as illustrated in Figure 1B, followed by several slow scans of cyclic voltammetry to detect any redox-active mediators generated by the biofilm for extracellular electron transfer. The eSPRi data were extracted from the recorded images as average pixel intensity within each grid square (Figure 1C).

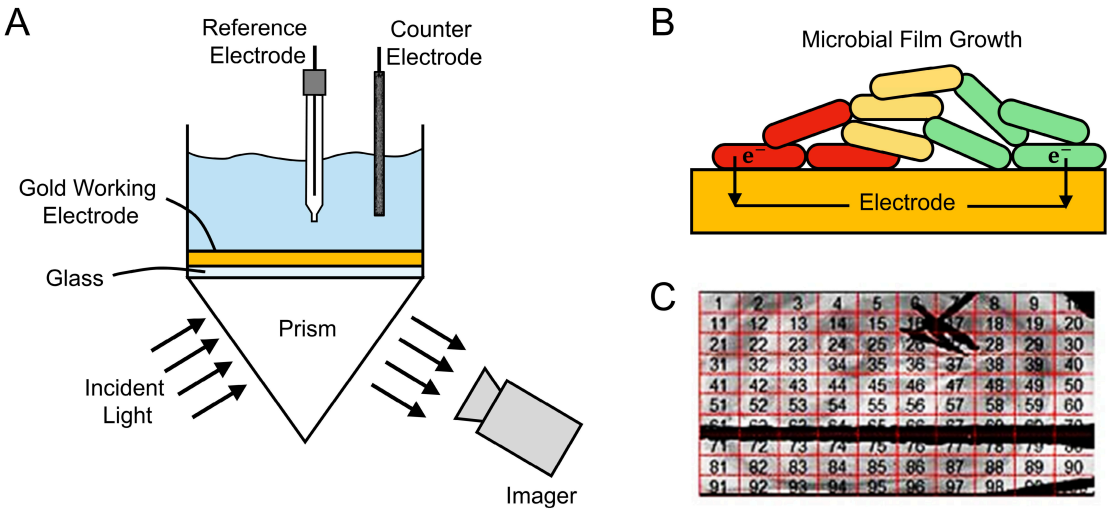


Figure 1. (**A**) Experimental design and setup of eSPRi. (**B**) Schematic of microbial biofilm growth on an electrode. (**C**) eSPRi image of the gold electrode showing the grid overlay for analysis.

The results of the first set of experiments are depicted in Figure 2. Figure 2A shows the complete dataset, comprising both eSPRi pixel intensity data from the middle of the image at square 45 and square 85 (Figure 1C), which is part of the gold film that is isolated and not electrically connected, along with electrochemical current data from the Gamry potentiostat. Additionally, Figure 2B illustrates representative cyclic voltammograms of eSPRi pixel intensity data and CV potentiostat measurements recorded at a scan rate of 2 mV per second.

In Figure 2, there are three time zones of interest highlighted. In the first zone, highlighted in orange, both the eSPRi signal and the electrochemical current increase, consistent with increasing biofilm-associated interfacial activity and current production during the early stage of the experiment. Early CVs in this region also show a small irreversible reduction peak centered near −0.075 V vs. SHE. The eSPRi response during these early CVs follows a similar trend. The gold film that is not electrically connected at square 85 does give an eSPRi signal that increases later in the experiment but to a

lower extent, suggesting an unspecified surface absorption, but well below the main eSPRi active signal.

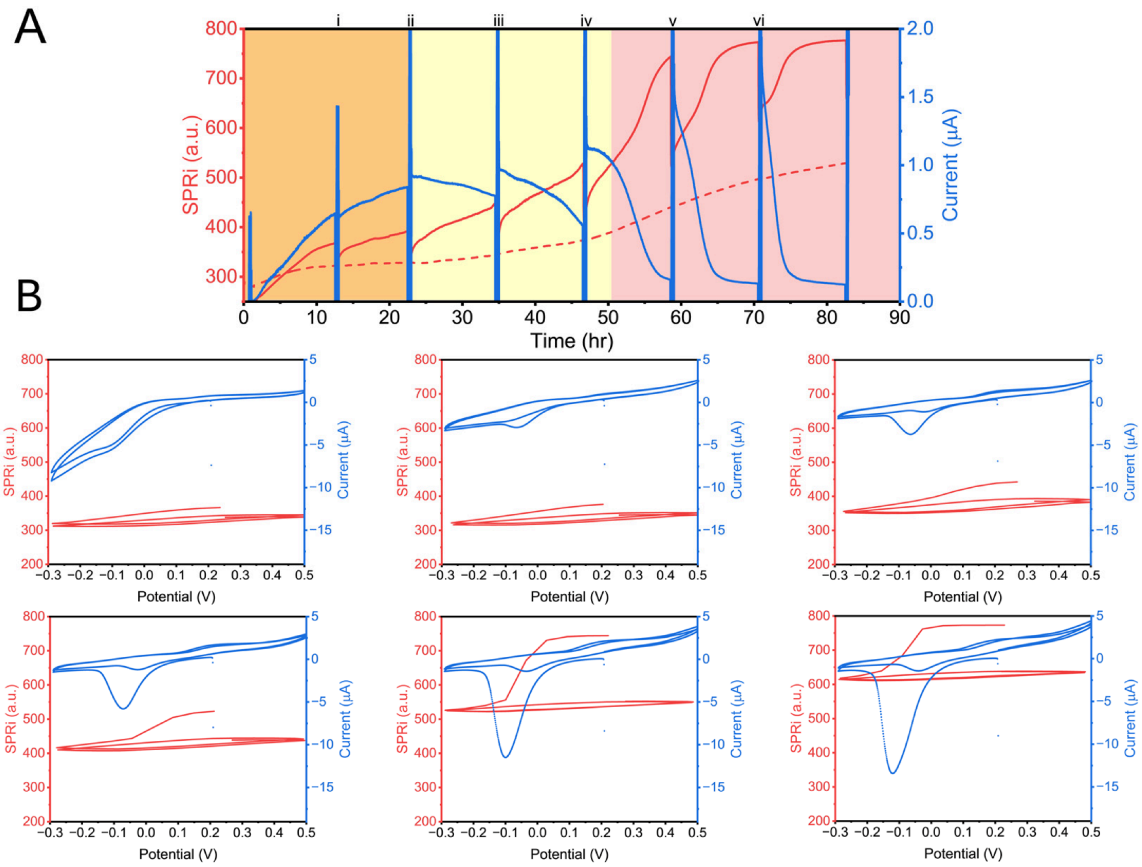


Figure 2. Biofilm activity of *Shewanella oneidensis* on gold electrodes. (**A**) eSPRi pixel intensity data and potentiostat current data vs. total time of the experiment measured at 0.31 V vs. SHE. (**B**) Cyclic voltammograms of eSPRi pixel intensity data and potentiostat data at time points shown in the figure, measured at a scan rate of 2 mV per second. The dashed line in Figure (**A**) represents isolated gold film that is not electrically connected (square #85 in Figure 1). All data were recorded under nitrogen in *Shewanella oneidensis* medium. The different highlighted time zones are discussed in the text.

In addition, in Supporting Material (Figure S1), we show a 2nd experimental replicate presenting a similar time zone of interest but also a series of square regions overlaid with their eSPRi signals, showing the variability of the absolute eSPRi signal intensity but very consistent behavior in the different time zones. The current did decrease earlier as compared to the previous experiment and an addition of lactate at 22.3 h didn't restore the signal, but the overall similar three time zones of interest are clearly seen.

In the second zone, highlighted in yellow, the electrochemical current begins to decrease while the eSPRi signal increases. CVs collected in this region show an increase in the irreversible reduction peak centered near −0.075 V vs. SHE. After one of these CV perturbations, there is a reset of both datasets, followed by a pattern similar to the beginning of Zone 2 with a decrease in electrochemical current and an increase in eSPRi signal.

In Zone 3, highlighted in pink, the trends become more pronounced with a larger decrease in current and a greater increase in eSPRi signal, along with later CVs showing an increase in the irreversible reduction peak centered near −0.075 V vs. SHE with a corresponding drop in the eSPRi signal. During this phase of the experiment, each CV is followed by an increased current and decreased eSPRi signal during the chronoamperomet-

ric period immediately after the CV ends. This is followed by a roughly 5 h period during which the eSPRi signal rises and the current falls.

Based on the distinct observation zones, our core observation is that current and eSPRi signals initially rise together, followed by a period where current falls while eSPRi rises, and finally, CV transiently perturbs both signals. One initial interpretation was that a cytochrome-flavin-associated interfacial state became progressively more oxidized as the experiment proceeded; however, the lactate measurements do not support bulk lactate depletion as the primary driver of this transition.

To assess whether bulk lactate depletion could explain the decline in current, we used High-Performance Liquid Chromatography (HPLC) to test lactate concentrations at the beginning of the experiment and at the point when the current dropped.

3.2. Lactate Consumption During Growth

In order to assess whether bulk lactate depletion accounted for the transition to a low-current state, HPLC analysis was conducted, and representative results from comparable runs are shown in Figure S2. Lactate concentration remained near the initial value of approximately 22.9 mM over the sampled interval (Figure S1), with no substantial decrease within the resolution of the method. These results indicate that bulk lactate depletion is unlikely to be the primary cause of the decline in current. These results suggest that the changes in chronoamperometric current and the shape of the CV were not driven primarily by bulk lactate consumption but instead reflect changing interfacial dynamics.

3.3. Mutant Strain Data

To further probe the origins of the interfacial signaling, we investigated the gold/protein interface with a mutant strain of *Shewanella oneidensis* MR-1, which has the genotype ΔmtrC ΔmtrA ΔmtrB ΔomcA (also known as Δmtr) [10]. This strain is deficient in key cytochromes associated with the canonical Mtr-mediated extracellular electron transfer pathway. The results are shown in the Supplementary Information in Figure S3. Over two days, this strain exhibited an initial lag but eventually generated current. Interestingly, the CVs of the mutant strain also displayed the irreversible peak observed in the wild-type *S. oneidensis* experiments. This suggests that the irreversible peak observed near -0.075 V vs. SHE does not straightforwardly represent the canonical Mtr cytochrome pathway but may instead arise from the accumulation or rearrangement of another reducible interfacial species on the gold surface.

4. Discussion

We have successfully used electrochemical surface plasmon resonance imaging to monitor *Shewanella oneidensis* biofilm growth and interfacial electrochemical behavior on gold electrodes, achieving real-time correlation between optical signals and electrochemical activity. In our experimental setup, biofilm-electrode interactions evolved through discernible phases: an initial attachment and growth phase with increasing current and eSPRi signal, followed by a phase with diminishing current generation even as the eSPRi signal remained elevated.

It is important to distinguish direct observations from what can be inferred. We observed that an irreversible reduction feature appears and grows, and that running a cyclic voltammogram transiently lowers the eSPRi signal and increases subsequent anodic current. Because the eSPRi intensity can reflect multiple properties such as changes in refractive index, biofilm thickness, extracellular material accumulation, and not just electron transfer, we approach the mechanism cautiously.

One possible explanation consistent with the present observations is that an uncharacterized species or conformational state binds or shifts at the gold interface, serving to limit continuous electron transfer from the biofilm to the bare gold. During the voltage sweep of the CV, this interfacial state is altered, or an interfacial redox pool is transiently perturbed, leading to the irreversible peak and the transiently recovered anodic current. This gold-surface blocking model acts as a working hypothesis, though alternative explanations such as localized mediator redistribution, optical drift, or complex bulk refractive index changes remain plausible. These findings have interesting implications for bioelectrochemical technologies. In microbial fuel cells and bioreactors, maximizing current output is often a key goal. Our results demonstrate that simply providing excess substrate does not always lead to sustained current, as biofilms can enter a low-current state or a state consistent with limited electron-transfer efficiency due to other factors.

5. Conclusions

These results demonstrate that eSPRi can serve as a useful complementary probe of biofilm-electrode interfacial dynamics on gold electrodes. Current and eSPRi signals do not always evolve in parallel, highlighting complex interactions at the surface. The data suggest that changing interfacial conditions is not explained by bulk lactate depletion alone, but the mechanism remains unresolved. The present data does not uniquely identify the origin of the optical signal or the mechanism responsible for the low-current state, and additional control and mechanistic experiments will be required.

eSPRi is a promising tool in the study of electroactive biofilms, but improvements such as higher imaging resolution and faster capture rates will be necessary to fully leverage its potential. Higher-resolution SPR imaging would allow us to track the surface attachment and growth of subsections of the biofilm or even of individual cells, which would be a valuable tool in understanding heterogeneity of both single-species and mixed biofilms. Faster SPR (e.g., SPR microscopy on a single spot at kHz rates) could potentially catch rapid electron transfer events.

In conclusion, the use of eSPRi to image living biofilms can help us gain insights that purely electrical measurements or end-point assays cannot offer. As we refine these techniques and integrate them with biological analyses, we move closer to unraveling the mechanisms that enable bacteria like *S. oneidensis* to power devices and remediate environments. Future work should incorporate abiotic controls, scan-rate-dependent cyclic voltammetry, potential-step experiments, electrochemical impedance spectroscopy (EIS), microscopy, and expanded spatial analysis to further decouple specific redox mechanisms from broader interfacial changes, especially when comparing bare gold to SAM-modified electrodes. Ultimately, a better understanding of biofilm extracellular electron transfer will inform the design of more efficient microbial fuel cells, sensors, and bioelectronic interfaces, where microbial communities are harnessed for beneficial outcomes.

Supplementary Materials: The following supporting information can be downloaded at: https://www.mdpi.com/article/10.3390/electrochem7040029/s1, Figure S1: Second experimental replicate; Figure S2: Lactate concentration at selected time points during biofilm formation; Figure S3: eSPRi of the *Shewanella oneidensis* MR-1 with the genotype ΔmtrC ΔmtrA ΔmtrB ΔomcA.

Author Contributions: Conceptualization, L.J.B., J.P.G. and S.A.T.; methodology, L.J.B., J.P.G., R.L.M., Z.T.J., M.D.Y. and S.A.T.; software, L.J.B. and M.D.Y.; formal analysis, L.J.B., J.P.G., R.L.M., Z.T.J., M.D.Y. and S.A.T.; investigation, L.J.B., J.P.G., R.L.M., Z.T.J., M.D.Y. and S.A.T.; writing—original draft preparation, L.J.B., J.P.G., R.L.M., Z.T.J. and S.A.T.; writing—review and editing, L.J.B., J.P.G., R.L.M., Z.T.J., M.D.Y. and S.A.T. All authors have read and agreed to the published version of the manuscript.

Funding: This research was funded by the NRL Nanoscience Institute and the Office of Naval Research through the NRL base program.

Data Availability Statement: The original contributions presented in this study are included in the article/Supplementary Materials. Further inquiries can be directed to the corresponding author.

Acknowledgments: During the preparation of this manuscript, the authors used AWS GPT-5.4 Gov for grammar review. The authors reviewed and edited the output and take full responsibility for the content of this publication.

Conflicts of Interest: The authors declare no conflicts of interest. The funders had no role in the design of the study; in the collection, analyses, or interpretation of data; in the writing of the manuscript; or in the decision to publish the results.

References

1. Peng, L.; You, S.J.; Wang, J.Y. Electrode potential regulates cytochrome accumulation on *Shewanella oneidensis* cell surface and the consequence to bioelectrocatalytic current generation. *Biosens. Bioelectron.* **2010**, *25*, 2530–2533. [CrossRef] [PubMed]
2. Marsili, E.; Baron, D.B.; Shikhare, I.D.; Coursolle, D.; Gralnick, J.A.; Bond, D.R. *Shewanella* secretes flavins that mediate extracellular electron transfer. *Proc. Natl. Acad. Sci. USA* **2008**, *105*, 3968–3973. [CrossRef] [PubMed]
3. Xu, S.; Jangir, Y.; El-Naggar, M.Y. Disentangling the roles of free and cytochrome-bound flavins in extracellular electron transport from *Shewanella oneidensis* MR-1. *Electrochim. Acta* **2016**, *198*, 49–55. [CrossRef]
4. Bao, H.; Zheng, Z.; Yang, B.; Liu, D.; Li, F.; Zhang, X.; Li, Z.; Lei, L. In situ monitoring of *Shewanella oneidensis* MR-1 biofilm growth on gold electrodes by using a Pt microelectrode. *Bioelectrochemistry* **2016**, *109*, 95–100. [CrossRef] [PubMed]
5. Kane, A.L.; Bond, D.R.; Gralnick, J.A. Electrochemical analysis of *Shewanella oneidensis* engineered to bind gold electrodes. *ACS Synth. Biol.* **2013**, *2*, 93–101. [CrossRef] [PubMed]
6. Guo, K.; Freguia, S.; Dennis, P.G.; Chen, X.; Donose, B.C.; Keller, J.; Gooding, J.J.; Rabaey, K. Effects of Surface Charge and Hydrophobicity on Anodic Biofilm Formation, Community Composition, and Current Generation in Bio-electrochemical Systems. *Environ. Sci. Technol.* **2013**, *47*, 7563–7570. [CrossRef] [PubMed]
7. LaBelle, E.; Bond, D.R. Cyclic voltammetry of electrode attached bacteria. In *Bioelectrochemical Systems: From Extracellular Electron Transfer to Biotechnological Application*; Rabaey, R., Ed.; IWA Publishing: London, UK, 2011.
8. Golden, J.; Yates, M.D.; Halsted, M.; Tender, L. Application of electrochemical surface plasmon resonance (ESPR) to the study of electroactive microbial biofilms. *Phys. Chem. Chem. Phys.* **2018**, *20*, 25648–25656. [CrossRef] [PubMed]
9. Pirbadian, S.; Barchinger, S.E.; Leung, K.M.; Byun, H.S.; Jangir, Y.; Bouhenni, R.A.; Reed, S.B.; Romine, M.F.; Saffarini, D.A.; Shi, L.; et al. Shewanella oneidensis MR-1 nanowires are outer membrane and periplasmic extensions of the extracellular electron transport components. *Proc. Natl. Acad. Sci. USA* **2014**, *111*, 12883–12888. [CrossRef] [PubMed]
10. Coursolle, D.; Gralnick, J.A. Reconstruction of Extracellular Respiratory Pathways for Iron(III) Reduction in *Shewanella Oneidensis* Strain MR-1. *Front. Microbiol.* **2012**, *3*, 56. [CrossRef] [PubMed]

Disclaimer/Publisher's Note: The statements, opinions and data contained in all publications are solely those of the individual author(s) and contributor(s) and not of MDPI and/or the editor(s). MDPI and/or the editor(s) disclaim responsibility for any injury to people or property resulting from any ideas, methods, instructions or products referred to in the content.